

Synchronization-based parameter estimation from time series

U. Parlitz and L. Junge

Drittes Physikalisches Institut, Universität Göttingen, Bürgerstraße 42-44, D-37073 Göttingen, Germany

L. Kocarev

Department of Electrical Engineering, Ss. Cyril and Methodius University, Skopje, P.O. Box 574, Republic of Macedonia

(Received 22 July 1996)

The parameters of a given (chaotic) dynamical model are estimated from scalar time series by adapting a computer model until it synchronizes with the given data. This parameter identification method is applied to numerically generated and experimental data from Chua's circuit. [S1063-651X(96)12912-3]

PACS number(s): 05.45.+b, 43.72.+q, 47.52.+j

I. INTRODUCTION

The synchronization of (unidirectionally) coupled dynamical systems is currently investigated very intensely, in particular due to its potential applications in communication (see [1–9]). In this paper we want to address the question how synchronization can be used for modeling and time series analysis. Assume that you have sampled a time series from some (chaotic) physical process and that you know the structure of the underlying equations but not the parameters and those state variables that have not been measured. The goal is to find the unknown parameters and variables. This problem can, for example, be tackled using multiple shooting methods [10] or related approaches [11]. However, with all these methods not only do the parameters occur in the algorithm as unknown quantities, but also the initial values of the trajectory segments between the sampling times. One therefore has to solve a high-dimensional minimization or fixed point problem. This can be simplified considerably if a synchronization mechanism is used that yields automatically the right values of the state variables. Hence, using synchronization the dimension of the minimization problem is reduced to the number of unknown model parameters. In this paper we describe an implementation of this general concept [7,12,13] and demonstrate its applicability using experimental data from Chua's circuit. In Sec. II the necessary notation and a method for achieving synchronization are introduced and illustrated using the Hénon map. Section III contains the numerical and experimental results obtained for an electrical circuit and in Sec. IV we summarize the results and discuss possible generalizations and improvements of the method.

II. CONSTRUCTING SYNCHRONIZING SYSTEMS BY ACTIVE-PASSIVE DECOMPOSITION

In the following we describe a rather general method for constructing synchronizing systems starting from a given (chaotic) dynamical system. In view of the following application for parameter estimation the basic ideas are discussed for discrete dynamical systems only. The generalization for continuous systems is straightforward and may be found, for example, in Ref. [6].

The basic idea of this synchronization method consists in a decomposition of a given (chaotic) system into an active

and a passive part, where different copies of the passive part synchronize when driven by the same active component. Consider an arbitrary N -dimensional discrete (chaotic) dynamical system,

$$\mathbf{x}^{n+1} = \mathbf{F}(\mathbf{x}^n; \mathbf{p}), \quad (1)$$

where \mathbf{p} denotes a parameter vector. The goal is to rewrite this autonomous system as a nonautonomous system that possesses certain synchronization properties. Formally, we may write

$$\mathbf{x}^{n+1} = \mathbf{f}(\mathbf{x}^n, \mathbf{s}^n; \mathbf{p}), \quad (2)$$

where \mathbf{s}^n is some vector valued function of time [14] given by

$$\mathbf{s}^n = \mathbf{h}(\mathbf{x}^n). \quad (3)$$

The pair of functions \mathbf{f} and \mathbf{h} constitutes a decomposition of the original system \mathbf{F} (see also the example that follows). The crucial point of this decomposition is that for suitable choices of the function \mathbf{h} any system

$$\mathbf{y}^{n+1} = \mathbf{f}(\mathbf{y}^n, \mathbf{s}^n; \mathbf{p}) \quad (4)$$

that is given by the *same* function \mathbf{f} , the *same* parameters \mathbf{p} , the *same* driving \mathbf{s}^n , but *different* variables \mathbf{y}^n , synchronizes with the original system (2), i.e., $\|\mathbf{x}^n - \mathbf{y}^n\| \rightarrow 0$ for $n \rightarrow \infty$. More precisely, synchronization of the pair of (identical) systems (2) and (4) occurs if the dynamical system describing the evolution of the difference $\mathbf{e}^n = \mathbf{y}^n - \mathbf{x}^n$

$$\mathbf{e}^{n+1} = \mathbf{f}(\mathbf{y}^n, \mathbf{s}^n) - \mathbf{f}(\mathbf{x}^n, \mathbf{s}^n) = \mathbf{f}(\mathbf{x}^n + \mathbf{e}^n, \mathbf{s}^n) - \mathbf{f}(\mathbf{x}^n, \mathbf{s}^n)$$

possesses a stable fixed point at the origin $\mathbf{e} = \mathbf{0}$. In some cases this can be proved using stability analysis of the linearized system for small \mathbf{e} ,

$$\mathbf{e}^{n+1} = D\mathbf{f}(\mathbf{x}^n, \mathbf{s}^n) \cdot \mathbf{e}^n.$$

or using (global) Lyapunov functions. In general, however, the stability has to be checked numerically using the fact that synchronization occurs if all conditional Lyapunov exponents [15] of the nonautonomous system (2) are negative. In this case system (2) is passive and the decomposition is

therefore called an *active-passive decomposition* (APD) of the original dynamical system (1).

As an example we shall now consider the Hénon map that is given by the map

$$\mathbf{F}(\mathbf{x}; \mathbf{p}) = \begin{pmatrix} 1 - a_x x_1^2 + b_x x_2 \\ x_1 \end{pmatrix} \quad (5)$$

with the parameters $\mathbf{p} = (a_x, b_x) = (1.4, 0.3)$. A possible APD of this chaotic system is

$$\mathbf{f}(\mathbf{x}, s; \mathbf{p}) = \begin{pmatrix} 1 - a_x s^2 + b_x x_2 \\ x_1 \end{pmatrix} \quad (6)$$

with

$$s = h(\mathbf{x}) = x_1^2. \quad (7)$$

Since the resulting linear system for the error dynamics

$$\mathbf{e}^{n+1} = \begin{pmatrix} 0 & b_x \\ 1 & 0 \end{pmatrix} \mathbf{e}^n$$

is stable for $b_x < 1$ any copy of the nonautonomous system (6) will synchronize with the drive signal s^n . Note that here and in the following we consider scalar drive signals only.

III. PARAMETER ESTIMATION

A. Hénon map

Until now we have assumed that the parameters \mathbf{p} of the drive system and the response system are the same. If this is not the case the ordinary or *identical synchronization* ($\mathbf{y} \rightarrow \mathbf{x}$) degrades and breaks down completely. However, as long as the response system is passive (i.e., it possesses negative conditional Lyapunov exponents) the so-called *generalized synchronization* [2,16,17] continues to occur. This means, that there exists a function \mathbf{H} such that in the limit $n \rightarrow \infty$ the state \mathbf{y} of the response system is given by $\mathbf{H}(\mathbf{x})$. Since the occurrence of generalized synchronization depends on the stability properties of the response system only, it is very robust with respect to parameter mismatch between drive and response [16]. Important for the following minimization approach is the fact that the existence of generalized synchronization leads here to a smooth dependence of the averaged synchronization error

$$E = \sqrt{\frac{1}{N} \sum_{n=1}^N [s^n - h(\mathbf{y}^n)]^2} \quad (8)$$

on the parameter mismatch. Of course, the error E has to be computed after the synchronization transient decayed and the response system has to remain passive upon parameter variation.

Let \mathbf{p} be the parameter vector of the drive and \mathbf{q} the parameter vector of the response. Then $E = E(\mathbf{p}, \mathbf{q})$ is a direct measure for the (dis-)agreement of the parameter values. Since the parameters of the drive are assumed to be fixed we will investigate in the following the error $E = E(\mathbf{q})$ as a function of \mathbf{q} .

Figure 1 shows as an example of the dependence of E on

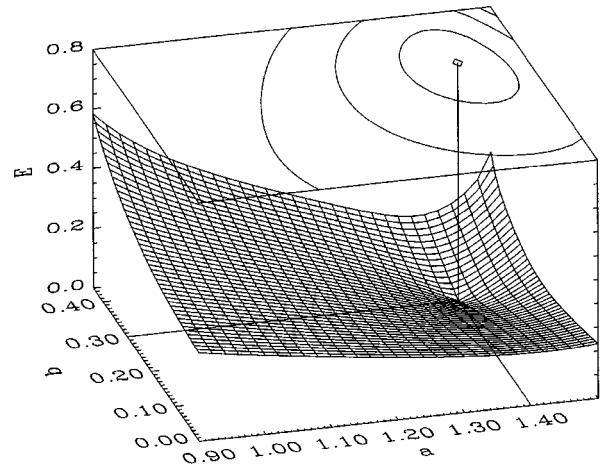


FIG. 1. Averaged synchronization error E vs response parameters (a_y, b_y) of the Hénon map.

$\mathbf{q} = (a_y, b_y)$ for two unidirectionally coupled Hénon maps (9) and (10):

$$\mathbf{x}^{n+1} = \mathbf{f}(\mathbf{x}^n, s^n; \mathbf{p}), \quad (9)$$

$$\mathbf{y}^{n+1} = \mathbf{f}(\mathbf{y}^n, s^n; \mathbf{q}), \quad (10)$$

where \mathbf{f} and s^n are given by Eqs. (6) and (7), respectively. As can be seen there is a very well pronounced minimum of E at $\mathbf{q} = \mathbf{p}$. In order to match the parameters of the response with those of the drive we thus need a strategy to minimize the synchronization error. This can be done using a general minimization routine, like the subroutine POWELL from Ref. [19] that we used for the computations presented in this paper. Figure 2(a) shows the parameters $\mathbf{q} = (a_y, b_y)$ of the driven “model” system (10) vs the number of line minimizations of the routine POWELL. As can be seen already after

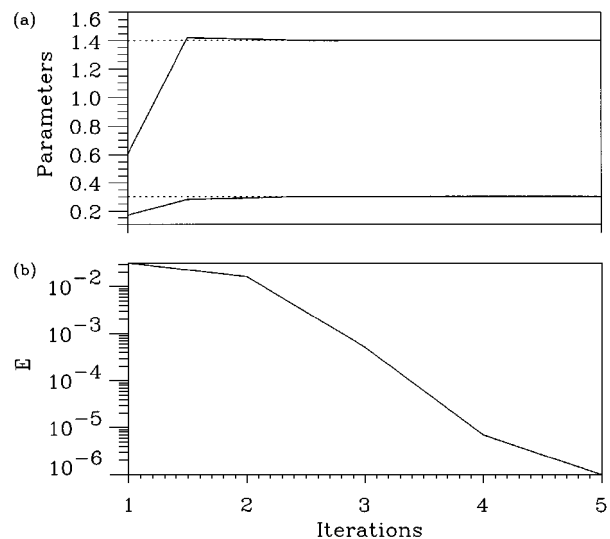


FIG. 2. Convergence of (a) the response parameters (a_y, b_y) of the driven Hénon map [Eq. (10)] and (b) the synchronization error E vs number of iterations of the routine used to minimize the synchronization error E [Eq. (8)]. The dotted lines in (b) give the exact parameter values $\mathbf{p}_x = (1.4, 0.3)$ of the driving Hénon map.

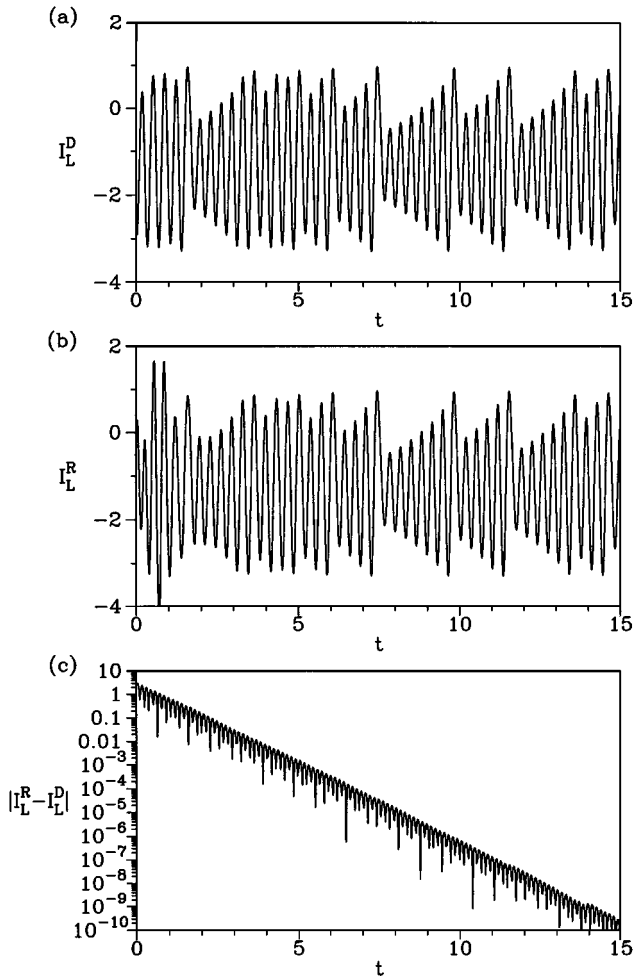


FIG. 3. Synchronization of two Chua circuits due to the sporadic V_{C1} coupling given by Eq. (15). Plotted are (a) the current I_L^D of the drive system, (b) the current I_L^R of the response system, and (c) the difference $|I_L^R - I_L^D|$ as a function of time t .

three iterations the true parameter values $\mathbf{p}=(1.4,0.3)$ are reached. The length of the time series used was $N=100$ where the first 30 values were used for the synchronization transient and the remaining 70 samples served for the estimation of the synchronization error (8). The decreasing synchronization error E is shown in Fig. 2(b). In our implementation of the search algorithm a search interval $[p_k^{\min}, p_k^{\max}]$ is used to prevent the minimization algorithm to use parameter values that are obviously wrong (for physical reasons, for example). This search interval is mapped to the real axis by the transformation

$$g(p_k) = \tan \left[\frac{\pi}{p_k^{\max} - p_k^{\min}} \left(p_k - \frac{p_k^{\max} + p_k^{\min}}{2} \right) \right].$$

Using this transformation the search process may get stuck near the boundaries p_k^{\min} and p_k^{\max} as long as it is moving in parameter regions far from the minimum. In those cases the minimization was reinitialized at a random position in the corresponding parameter interval.

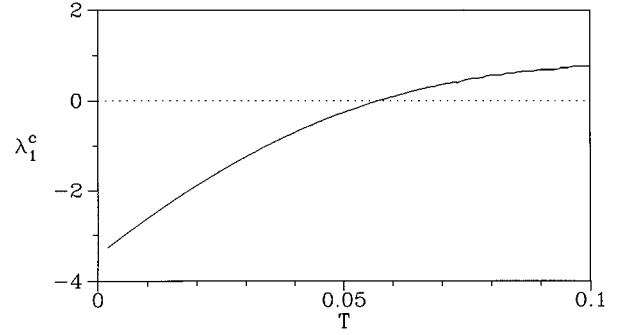


FIG. 4. Largest conditional Lyapunov exponent λ_1^c of the sporadically driven Chua circuit vs coupling time T .

B. Chua's circuit

The second and main example of this paper is Chua's circuit [18] that is given by the following set of equations:

$$\begin{aligned} C_1 \frac{dV_{C1}}{dt} &= G(V_{C2} - V_{C1}) - g(V_{C1}), \\ C_2 \frac{dV_{C2}}{dt} &= G(V_{C1} - V_{C2}) + I_L, \\ L \frac{dI_L}{dt} &= -V_{C2} - R_0 I_L, \end{aligned} \quad (11)$$

where g is a piecewise-linear function defined by

$$g(V) = m_0 V + \frac{1}{2}(m_1 - m_0)[|V + B_p| - |V - B_p|]. \quad (12)$$

For the numerical simulations of the circuit we used the parameter values $m_0 = -0.405$ mS, $m_1 = -0.756$ mS, $G = 1/R$ with $R = 1700 \Omega$, $B_p = 1.08$ V, $L = 18$ mH, $R_0 = 20 \Omega$, $C_1 = 10$ nF, and $C_2 = 100$ nF. Integration of this set of differential equations generates a flow $\phi^t: \mathbb{R}^3 \rightarrow \mathbb{R}^3$ and for fixed $t = T$ we may consider this system as a time discrete system or iterated map

$$\begin{aligned} F &= \phi^T: \mathbb{R}^3 \rightarrow \mathbb{R}^3 \\ \mathbf{x} &\rightarrow \phi^T(\mathbf{x}) \end{aligned} \quad (13)$$

with

$$\mathbf{x} = (V_{C1}, V_{C2}, I_L). \quad (14)$$

The APD approach for establishing synchronization is now applied to this discrete system. In view of the following application we consider the case that a time series $\{s^n\}$ is obtained from Chua's circuit by sampling the voltage V_{C1} at discrete times $t_n = nT$, i.e., $s^n = V_{C1}(t_n)$. The APD consists in a replacement of the V_{C1} variable in the model at times t_n and is formally given by

$$\mathbf{x}^{n+1} = \mathbf{f}(\mathbf{x}^n, s^n; \mathbf{p}) = \phi^T(s^n, x_2^n, x_3^n), \quad (15)$$

where $\mathbf{x}^n = (x_1^n, x_2^n, x_3^n) = (V_{C1}, V_{C2}, I_L)(t_n)$ and \mathbf{p} denotes the set of all parameters of Chua's circuit. To study synchronization two Chua's circuits, drive and response, are consid-

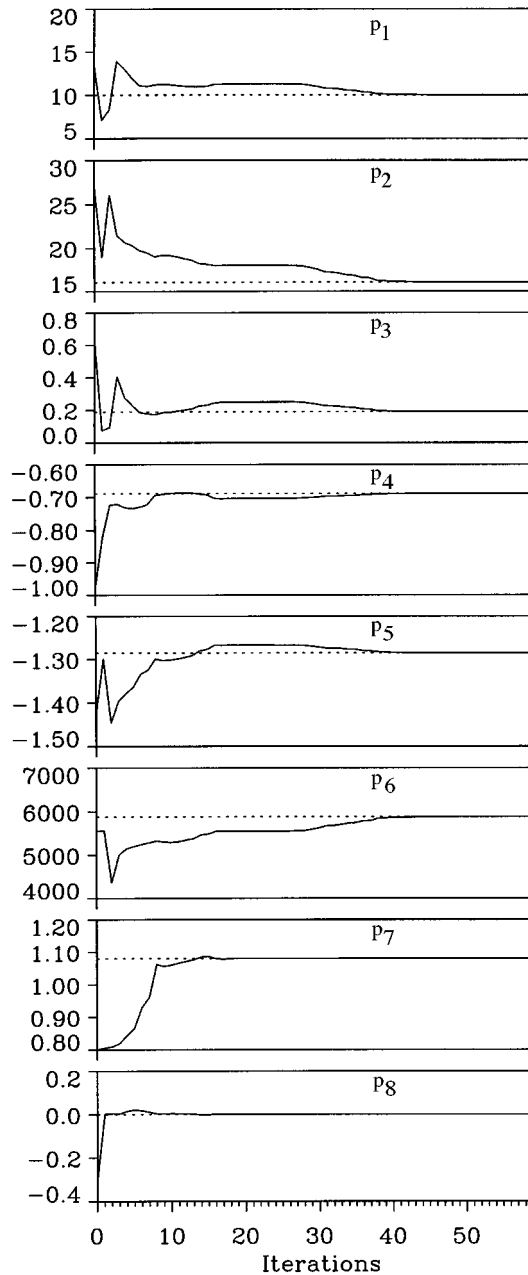


FIG. 5. Convergence of the normalized parameters (16) during the minimization process for a numerically generated V_{C1} time series. The dotted lines give the values of the drive system used for computing the time series.

ered with parameter vectors \mathbf{p} and \mathbf{q} , respectively. If the parameters of the drive system and the response system agree exactly this type of unidirectional *sporadic coupling* [8,9] leads to perfect synchronization although both continuous systems oscillate freely during the time intervals between the coupling. This is illustrated in Fig. 3 for a coupling time of $T=0.025$ ms.

To investigate the synchronization properties as a function of the coupling time T we have computed the largest conditional Lyapunov exponent of the sporadically driven system (13). As can be seen in Fig. 4 λ_1^c is negative for $T \in [0, 0.057]$. For these T values we thus can achieve synchronization with this particular type of coupling.

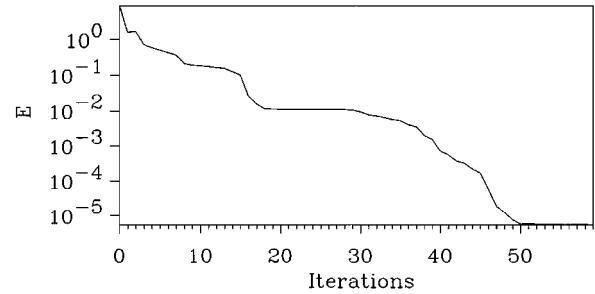


FIG. 6. Synchronization error E vs number of iterations of the minimization algorithm for the numerically generated V_{C1} time series from Chua's circuit (compare Fig. 5).

We shall now assume again that the parameter values of the driving circuit are unknown and the parameter dependence of the synchronization error E given by Eq. (8) will be used to identify these values. As in the case of the Hénon map the minimization routine POWELL from Ref. [19] is used to reduce the synchronization error in order to find the correct parameter values. Simultaneously, the largest conditional Lyapunov exponent of the response system is monitored to make sure that the “model system” doesn't lose its ability to synchronize with the driving time series.

For the search of the smallest synchronization error all eight parameters in Eqs. (11) and (12) have been varied by the minimization routine POWELL [19]. Additionally, a possible offset b and an amplification factor a upon measurement have also been taken into account in the minimization process, i.e., we assume

$$s^n = a[V_{C1}(t_n) - b].$$

Varying the factor a , however, is equivalent to changes of the breakpoint voltage B_p . Therefore, we used B_p to take into account a possible amplification and the minimization problem solved was nine dimensional [eight parameters from Eqs. (11) and (12) and the offset b]. Since the parametrization of Eqs. (11) and (12) is redundant the following eight normalized parameters have been computed from the nine parameters used in the minimization routine:

$$\begin{aligned} p_1 &= C_2/C_1 = 10, & p_2 &= R^2 C_2/L \approx 16, \\ p_3 &= RR_0 C_2/L \approx 0.189, & p_4 &= m_0 R \approx -0.689, \\ p_5 &= m_1 R \approx -1.285, & p_6 &= 1/RC_2 \approx 5882, \\ p_7 &= B_p, & p_8 &= b, \end{aligned} \quad (16)$$

where p_6 and p_7 give the time scaling and the amplitude scaling, respectively. Of course, one can also minimize the synchronization error with respect to the normalized parameters (16). This alternative, however, turned out to be less stable and efficient.

First, we consider a numerically generated V_{C1} time series using Eqs. (11) and (12) with the parameter values given above, an amplification factor of one and no offset ($b=0$). The time series was sampled with 40 kHz and consists of 1500 samples, where the first 500 values are used for the synchronization transient and the last 1000 samples for computing the averaged synchronization error E [Eq. (8)]. For this time series the search algorithm converges to the exact

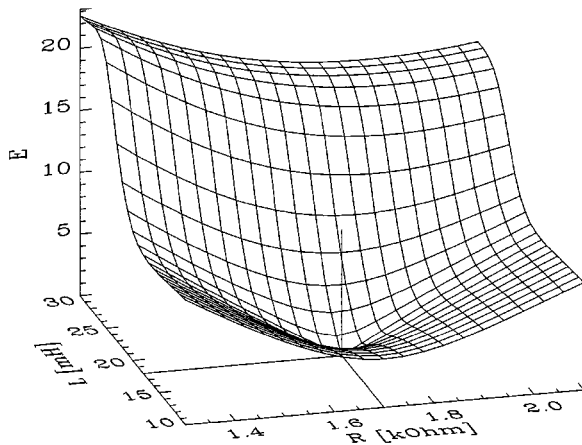


FIG. 7. Synchronization error E vs value of the resistor R and value of the inductance L for the numerically generated V_{C1} time series. The other parameters of the response circuit coincide with those of the drive.

values already after a few iterations and the synchronization error E vanishes as can be seen in Fig. 5 and Fig. 6.

In order to visualize the error landscape in the nine-dimensional parameter space we have plotted two-dimensional cross sections where the remaining seven parameters have been kept fixed at the exact values of the drive system. Figure 7 and Fig. 8 show two representative examples. In Fig. 7 the synchronization error E [Eq. (8)] is given vs the resistor R and the inductance L . As can be seen a clear minimum exists. Figure 8 shows the error E in the L - m_0 plane. Still a minimum exists, but in this case it is located in a rather flat valley and is thus more susceptible to any disturbances due to noise or model inaccuracies.

We turn now to experimental data taken from a hardware implementation of Chua's circuit. The V_{C1} time series used had a length of 10 000 samples and was sampled with 44 100 kHz. Figure 9 shows the convergence of the normalized parameters during the minimization process. The resulting es-

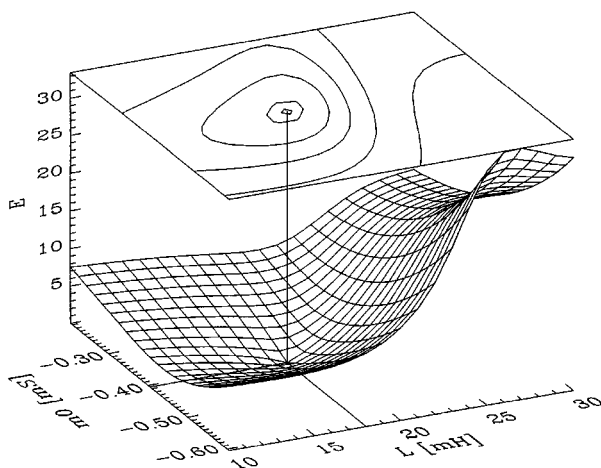


FIG. 8. Synchronization error E vs value of the inductance L and value of the slope m_0 for the numerically generated V_{C1} time series. The other parameters of the response circuit coincide with those of the drive.

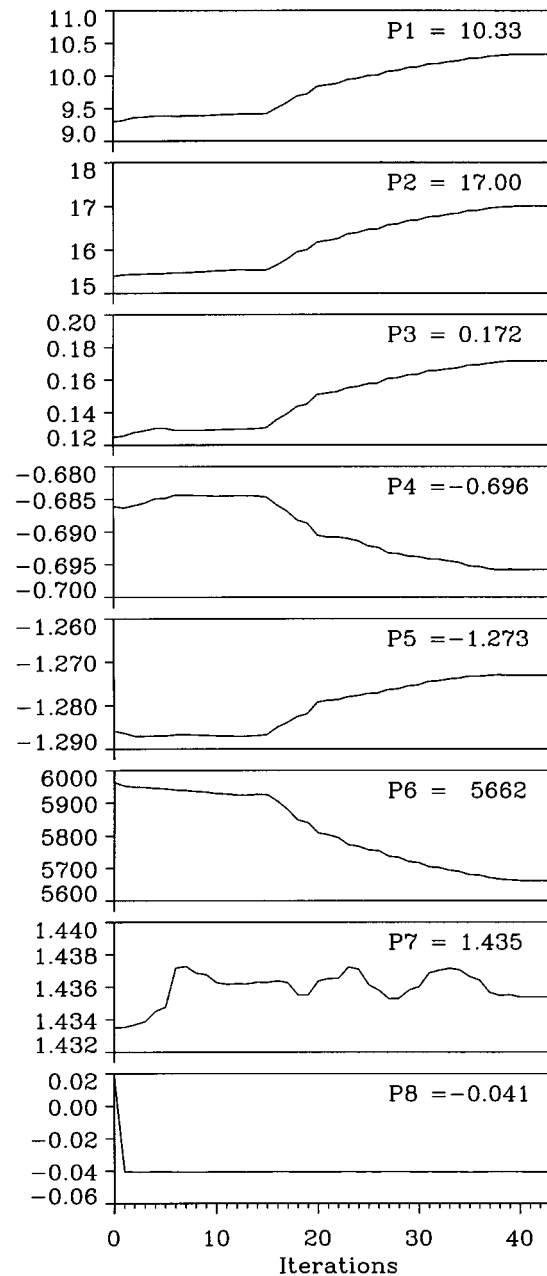


FIG. 9. Convergence of the normalized parameters (16) during the minimization process for an experimentally generated V_{C1} time series.

imates of the parameter values are given in the diagrams. In this case the minimum of the synchronization error is larger than zero due to the noise as can be seen in Fig. 10. Numerical simulations including noise have shown that noise with $SNR < 60$ dB may shift the minimum from the correct point in parameter space to some other location nearby. This means that a response system with slightly different parameter values as the drive fits better to the *noisy* data that are available.

In order to compare the experimentally observed dynamics and the model a V_{C1} time series has been generated using Eqs. (11) and (12) and the estimated parameter values. Figure 11 shows delay reconstructions of the attractors from the experimental data (solid curve) and the numerically gener-

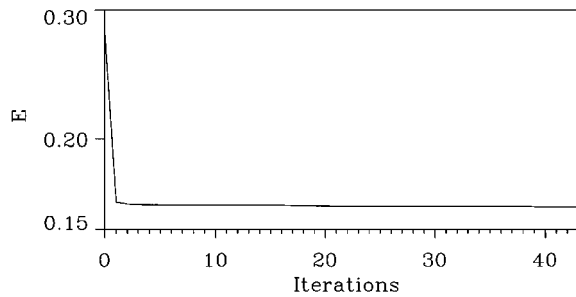


FIG. 10. Synchronization error E vs number of iterations of the minimization algorithm for the experimentally measured V_{C1} time series from Chua's circuit (compare Fig. 9).

ated time series (dashed curve). As can be seen both attractors are located in the same region of state space and look very similar, indicating a good agreement of the model dynamics and the experiment. This comparison can be extended to include invariants such as dimensions, Lyapunov exponents, or the topological organization of (unstable) periodic orbits [20].

IV. CONCLUSION

In this letter we have presented a parameter estimation method that recovers the parameter values of a given model from a single time series by minimizing an averaged synchronization error. Using time series from the Hénon map and Chua's circuit it was demonstrated that the error landscape is a sufficiently smooth function with a deep minimum at the true parameter values. For numerically generated time series this minimum and the corresponding correct parameter values were found already after a few iterations of the minimization routine. Similar results have been obtained for other dynamical systems such as the Lorenz system and a driven damped pendulum. In the case of real data (including noise) the minimum of the synchronization error landscape is less deep and may also be slightly shifted. Nevertheless, a comparison of attractor reconstructions from the experimental data and a numerical time series using the estimated parameter values yielded a satisfying agreement.

In comparison with similar approaches for synchronization-based parameter estimation [12,13] our method (i) is stable even when all parameters are estimated,

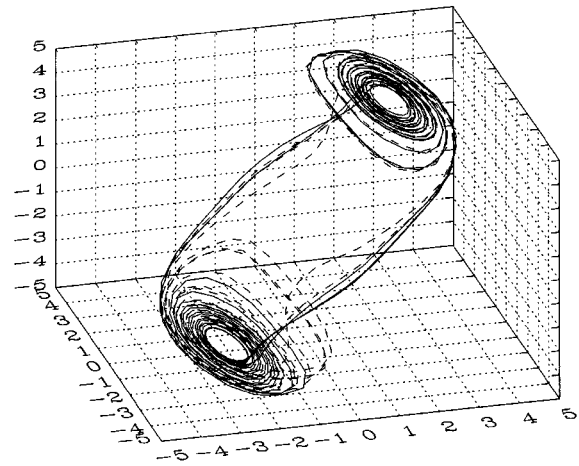


FIG. 11. Attractor reconstruction using delay embedding of the experimental data (solid curve) and a numerically generated V_{C1} time series based on the estimated parameter values (dashed curve).

(ii) can be used with discretely sampled time series, (iii) gives exact results when used with numerically generated data, and (iv) was shown to work well even for experimental data.

A possible application of this parameter estimation method is, for example, VLSI implementations of electronic systems like Chua's circuit where the determination of the actual values of the individual components is very difficult. In those cases where a continuous coupling between the experiment and a computer model is possible, similar methods may be applied where additional differential equations for the unknown parameters are used to control the adaption process [21,22]. The approach used there to derive the necessary parameter ODE's can in principle be generalized to the case of discrete dynamics that is considered in this paper. For further improvements and generalizations one may try different definitions of the synchronization error (cost function) or more efficient minimization algorithms.

ACKNOWLEDGMENTS

The authors thank C. Merkwirth, T. Stojanovski, M. Wiesenfeldt, and W. Lauterborn for stimulating discussions and support. This work was supported by a binational German-Macedonian project (No. MAK-004-95).

-
- [1] H. Fujisaka and T. Yamada, *Prog. Theor. Phys.* **69**, 32 (1983).
 - [2] V.S. Afraimovich, N.N. Verichev, and M.I. Rabinovich, *Radiophys. Quantum Electron.* **29**, 795 (1986).
 - [3] L. Pecora and T. Carroll, *Phys. Rev. Lett.* **64**, 821 (1990).
 - [4] K.M. Cuomo and A.V. Oppenheim, *Phys. Rev. Lett.* **71**, 65 (1993).
 - [5] C.W. Wu and L.O. Chua, *Int. J. Bifurc. Chaos* **4**, 979 (1994).
 - [6] L. Kocarev and U. Parlitz, *Phys. Rev. Lett.* **74**, 5028 (1995); U. Parlitz, L. Kocarev, T. Stojanovski, and H. Preckel, *Phys. Rev. E* **53**, 4351 (1996).
 - [7] R. Brown, N.F. Rulkov, and E.R. Tracy, *Phys. Rev. E* **49**, 3784 (1994).
 - [8] R.E. Amritkar and N. Gupte, *Phys. Rev. E* **47**, 3889 (1993).
 - [9] T. Stojanovski, L. Kocarev, and U. Parlitz, *Phys. Rev. E* **54**, 2128 (1996).
 - [10] E. Baake, M. Baake, H.G. Bock, and K.M. Briggs, *Phys. Rev. A* **42**, 5524 (1992).
 - [11] J.L. Breeden and A. Huebler, *Phys. Rev. A* **42**, 5817 (1990).
 - [12] R. Dedieu and M. Ogorzalek, *SPIE Proc. Vol. 2612*, 148 (1995).
 - [13] R. Caponetto, L. Fortuna, G. Manganaro, and M.G. Xibilia, *SPIE Proc. 2612*, 48 (1995).
 - [14] Generalizations like $\mathbf{s}^{n+1} = \mathbf{h}(\mathbf{x}^n, \mathbf{s}^n)$ are possible but will not be considered in this paper.

- [15] The technical notion of conditional Lyapunov exponents was introduced by Pecora and Carroll (Ref. [3]) in order to study the synchronization of subsystems.
- [16] L. Kocarev and U. Parlitz, *Phys. Rev. Lett.* **76**, 1816 (1996).
- [17] N.F. Rulkov, K.M. Sushchik, L.S. Tsimring, and H.D.I. Abarbanel, *Phys. Rev. E* **51**, 980 (1995).
- [18] *Chua's Circuit: A Paradigm for Chaos*, edited by R.N. Madan, World Scientific Series on Nonlinear Sciences, Series B, Vol. 1 (World Scientific, Singapore, 1993).
- [19] W.H. Press, B.P. Flannery, S.A. Teukolsky, and W.T. Vetterling, *Numerical Recipes* (Cambridge University Press, Cambridge, 1986).
- [20] C. Letellier, L. Le Sceller, P. Dutertre, G. Gouesbet, Z. Fei, and J.L. Hudson, *J. Phys. Chem.* **99**, 7016 (1995).
- [21] U. Parlitz, *Phys. Rev. Lett.* **76**, 1232 (1996).
- [22] U. Parlitz and L. Kocarev, *Int. J. Bifurc. Chaos* **6**, 581 (1996).